SCIENCE CHINA
Life Sciences

• RESEARCH PAPER •

December 2013 Vol.56 No.12: 1124–1133
doi: 10.1007/s11427-013-4569-y

A cellular response protein induced during HSV-1 infection inhibits viral replication by interacting with ATF5

WU LianQiu[1], ZHANG XueMei[1], CHE YanChun[1], ZHANG Ying[1], TANG SongQing[1], LIAO Yun[1], NA RuiXiong[1], XIONG XiangLin[2], LIU LongDing[1] & LI QiHan[1*]

[1]*Yunnan Key Laboratory of Vaccine Research & Development on Severe Infectious Diseases, Institute of Medical Biology, Chinese Academy of Medical Sciences & Peking Union Medical College, Kunming 650118, China;*
[2]*Kunming Medical University, Kunming 650032, China*

Received May 15, 2013; accepted September 5, 2013

Studies of herpes simplex virus type 1 (HSV-1) infection have shown that many known and unknown cellular molecules involved in viral proliferation are up-regulated following HSV-1 infection. In this study, using two-dimensional polyacrylamide gel electrophoresis, we found that the expression of the HSV-1 infection response repressive protein (HIRRP, GI 16552881) was up-regulated in human L02 cells infected with HSV-1. HIRRP, an unknown protein, was initially localized in the cytoplasm and then translocated into the nucleus of HSV-1-infected cells. Further analysis showed that HIRRP represses HSV-1 proliferation by inhibiting transcription of the viral genome by interacting with the cellular transcription factor, ATF5, via its N-terminal domain. ATF5 represses the transcription of many host genes but can also act as an activator of genes containing a specific motif. We found that ATF5 promotes the proliferation of HSV-1 via a potential mechanism by which ATF5 enhances the transcription of viral genes during the course of an HSV-1 infection; HIRRP then induces feedback repression of this transcription by interacting with ATF5.

herpes simplex virus type 1 (HSV-1), HSV-1 infection response repressive protein (HIRPP), ATF5, transcriptional regulation

Citation: Wu L Q, Zhang X M, Che Y C, et al. A cellular response protein induced during HSV-1 infection inhibits viral replication by interacting with ATF5. Sci China Life Sci, 2013, 56: 1124−1133, doi: 10.1007/s11427-013-4569-y

Herpes simplex virus type 1 (HSV-1) infections are frequently impaired by molecules that are induced at different phases by specific cellular responses to virus infection [1,2]. This implies that many HSV-1 virions are required to maintain the infectious state and that they facilitate the survival of the virus through interactions with various cellular molecules [3,4]. A variety of specific gene transcription regulatory mechanisms are active during the course of HSV-1 infection. Interactions between viral and cellular molecules generate a specific microenvironment during HSV-1 infection [5,6], leading to either lytic or latent infections in different host cells [7–13].

When HSV-1 enters the epithelium, *cis*-activation of the viral genome is triggered by a specific motif (TgACgTCAA) in the promoter region of the viral immediate early (IE) gene. This motif is recognized by the tegument protein (VP16) in conjunction with the host proteins Oct1 and HCF. This *cis*-activation event induces the sequential transcription of IE, early (E) and late genes [14–16] and leads to a lytic infection [17]. With respect to the entry of HSV-1 into neural cells, a deficiency in the Oct1 transcription factor is likely to contribute to the silencing of viral genes [18], subsequently affecting the production of the viral RNA latency-associated transcript (LAT) [19]. Although these find-

*Corresponding author (email: liqihan@imbcams.com.cn)

ings reveal some basic features of HSV-1 infection [20], the details of the molecular mechanisms involved remain unclear. HSV-1 infection studies involving mRNA differential display reverse transcription polymerase chain reaction (RT-PCR), 2D electrophoresis and microRNA analyses have provided further insights [21–23]. These studies revealed that many more cellular and viral molecules, including viral RNAs, are involved in the initial stages of HSV-1 infection than previously thought [24,25]. During these initial stages, the expression of certain cellular molecules is up-regulated as part of the host immune response; these molecules then activate viral transcription and interfere with viral proliferation. Molecules encoded by the viral genome are associated with its replication activity [26].

The expression levels of some of these functional viral and cellular proteins are up-regulated in human fibroblasts following HSV-1 infection [27–29]. Several cellular molecules have negative functions with respect to the regulation of viral gene transcription. This differs from the conventional interferon response, which restricts viral replication by affecting the cellular transcriptional regulatory system [21,30,31]. In this study, we aimed to determine which cellular and viral molecules are involved in the transcriptional regulation of HSV-1.

1 Materials and methods

1.1 Cells and viruses

The L02 (human liver), Vero (African green monkey kidney), HeLa (human cervical carcinoma) and 293T (human kidney) cell lines were obtained from the ATCC (Manassas, VA, USA) and maintained in Dulbecco's modified Eagle's medium (DMEM; Highclone, Grand Island, NY, USA) supplemented with 10% fetal calf serum (FCS). The HSV-1 F strain was maintained by the Institute of Medical Biology, Chinese Academy of Medical Sciences. Virus samples (100 μL) that had been serially diluted 10-fold were added to the wells of 96-well culture plates containing Vero cells (1×10^4 cells/well). The plates were incubated at 37°C/5% CO_2 for 6–7 d, until viral cytopathic effects (CPE) were assessed. Greater than 50% CPE was considered to be indicative of viral infection.

1.2 Virus titration

For virus adsorption, virus stocks (1 mL) were serially diluted 10-fold (1∶10–1∶100000), and 500 μL of the diluted stocks was added to wells of 6-well plates that had been coated with Vero cells for 1 h. Pre-warmed 2× DMEM was added to a 1∶1 mixture of 2% (w/v) agarose and 2% (w/v) agar. This mixture was then added to the wells containing adsorbed virus, and the plates were incubated at 37°C for 4–5 d until plaque formation was observed. We added 1.5 mL of 4% (w/v) paraformaldehyde to each well and incubated the plates at room temperature for 1 h; 0.5% (w/v) crystal violet was added to assist with visualizing the plaques.

1.3 Plasmid generation

All primers used in this study are listed in Table 1. The *hirrp* gene, encoding the HSV-1 infection response repressive protein (HIRRP), was amplified using cDNA reverse transcribed from the total RNA of infected 293 cells as a template. Total RNA was extracted from the infected cells using a Qiagen RNeasy Mini Kit (Qiagen, Hilden, Germany) and reverse-transcribed using a Quantscript RT Kit (TIANGEN, China). Two specific primers were used (HIRRP-F and HIRRP-R; Table 1), and the resulting amplicon was digested with the *Eco*R I and *Xho* I restriction endonucleases and cloned into the pcDNA3 plasmid vector (Invitrogen, Carlsbad, CA, USA) to generate pcDNA3-HIRRP. We digested pcDNA3-HIRRP with *Eco*R I and *Sal* I and cloned the products into pEGFP-N2 (Clontech, Palo Alto, CA, USA) to create pGEFP-HIRRP. This vector was then subjected to digestion with *Eco*R I and *Sal* I, and the products were cloned into pGEX-5X-1 (Amersham, Piscataway, NJ, USA) to generate pGEX-HIRRP. The pGEX-HIRRP plasmid was digested with *Eco*R I and *Sal* I, and the resulting products were cloned into pGBKT7 (Clontech, Palo Alto, CA, USA) to yield pGBKT7-HIRRP.

Table 1 Primers used in this study

Primers	Amplicon
F: AATGAATTCATGGAGCGGCTCCGGGAGC R: ATAGTCGACAGCCTGCTCTCAGCTTTTG	*hirrp*
F: AATGAATTCATGGAGCGGCTCCGGGAGC R: ATACTCGAGTCAGCCTGCTCTCAGCTTT	*hirrp-N*
F: AATGAATTCATGCTGGGGATCCGGCAGC R: ATACTCGAGTCAGCCTGCTCTCAGCTTT	*hirrp-C*
F: GTGCATGAAAACCTGGATGC R: TTGCCCGTCCAGATAAAGTC	*icp0*
F: CAGCAAGAAGCCACGGAAGT R: GCGTCGGTCACGGCATAA	*tk*
F: CCGATGCCGGTTTCGGAAT R: CCCATGGAGTAACGCCATATCT	*gc*
F: CTGGTCAGCTTTCGGTACGA R: CAGGTCGTGCAGCTGTTTGC	*gb*
F: GGCATCTCACCCTGAAGTA R: GGGGTGTTGAAGGTCTCAAA	*β-actin*
F: AATGAATTCATGTCACTCCTGGCGA R: ATACTCGAGAGCAGCTACGGGTCCT	*atf5*
F: AATGAATTCATGATCTACTGCCGCAACG R: ATACTCGAGAGCAGCTACGGGTCCT	*atf5-c*
F: AGAAGUCUGUCAUGCUCAAGU R: UUGAGCAUGACAGACUUCUGC	*Hirrp* RNAi fragments

A fragment of the N-terminus of the *hirrp* gene (nucleotides 1–420) was amplified using primers HIRRP-N-F and HIRRP-N-R (Table 1). The amplicon was digested with *Eco*R I and *Xho* I, and the resulting products were cloned into pcDNA3 to give pcDNA3-HIRRP-N. A fragment of the C-terminus of the *hirrp* gene (nucleotides 241–630) was amplified using primers HIRRP-C-F and HIPPR-C-R (Table 1). The amplicon was digested with *Eco*R I and *Xho* I and cloned into pcDNA3 to obtain the pcDNA3-HIRRP-C plasmid.

An *atf5* gene fragment encoding the ATF5 protein was amplified by polymerase chain reaction (PCR) using DNA from 293 cells as a template and primers ATF5 F and ATF5 R. The resulting PCR products were digested with *Eco*R I and *Xho* I and cloned into pcDNA3 to generate pcDNA3-ATF5. This plasmid was then digested with *Eco*R I and *Xho* I and cloned into pGADT7 (Clontech, Palo Alto, CA, USA) to produce pGADT7-ATF5. The portion of *atf5* encoding amino acids 163–283 of ATF5 was amplified using primers ATF5 C-F and ATF5 C-R; the resulting amplicon was digested with *Eco*R I and *Xho* I and cloned into pGADT7 to generate pGADT7-ATF5-C.

1.4 Cell transfection

Cells were grown to approximately 80% confluence; the culture medium was then aspirated, and the cells were washed twice with phosphate-buffered saline (PBS). Lipofectamine 2000 (2 μL; Invitrogen, Carlsbad, CA, USA) and plasmid DNA (0.8 μg) were diluted separately in DMEM lacking FCS and antibiotics and then thoroughly mixed and incubated at 37°C for 20 min before being added to the cells. The cell cultures were incubated with the transfection mixtures at 37°C for 6 h. The transfection mixtures were then aspirated and replaced with normal growth media.

1.5 Immunofluorescence assays

Cells grown to approximately 70% confluence in 24-well plates were infected with HSV-1 at a multiplicity of infection (MOI) of 0.1. Cells at 24 and 48 h post-infection (hpi) were fixed with pre-chilled 4% paraformaldehyde in PBS at room temperature for 15 min. The cells were permeabilized with PBS containing 0.2% (v/v) Triton X-100 for 10 min and then blocked with PBS containing 1% (w/v) bovine serum albumin (BSA; PBS-BSA buffer) for 60 min. The cells were incubated with HIRRP anti-serum overnight at 4°C and washed with PBS-BSA, followed by incubation with a FITC-labeled anti-mouse antibody (1∶20000, Abcam, Cambridge, UK) at room temperature for 30 min. The cells were observed using a fluorescence microscope.

1.6 Northern blot analysis

Total cellular RNA was extracted from HSV-1-infected L02 cells (MOI=0.1) at 6 and 12 hpi using TRIZOL (Invitrogen, Carlsbad, CA, USA). The extracted RNA was subjected to denaturing electrophoresis in 1% formaldehyde and transferred to a nylon membrane for hybridization with γ-^{32}P-labeled probes (PerkinElmer, Wellesley, MA, USA). The 18S rRNA was used as an internal control. X-ray autoradiography was conducted according to the manufacturer's recommendations (Thermo Scientific, Rockford, IL, USA).

1.7 Quantitative PCR (qPCR)

Extracted cellular total RNA (TaKaRa, Japan) was reverse-transcribed into cDNA (Promega, Madison, WI, USA). The mRNAs encoding HIRRP, ICP0, TK, gC, gB and β-actin (reference gene) were amplified using the appropriate cDNA as a template for the Real Master Mix (SYBR Green) PCR system (TaKaRa, Japan). The thermal cycling parameters involved an initial denaturation step at 95°C for 3 min, followed by 35 cycles of 95°C for 10 s, 56°C for 1 min, and 68°C for 40 s. Each experiment was repeated three times, with expression levels quantified using the $2^{-\triangle\triangle C_T}$ method, where C_T indicates the cycle threshold [32]. The data were analyzed using GraphPad Prism 4.0 (GraphPad Software Inc., San Diego, CA, USA) with values presented as mean±standard error (SE) of three replicate samples.

1.8 Western blot analysis

L02 cells were grown to 80%–90% confluence and infected with HSV-1 at an MOI of 0.1. The cells were harvested at 0, 12, 24, 36, and 48 hpi and lysed in RIPA buffer (50 mmol L^{-1} Tris-HCl, 150 mmol L^{-1} NaCl, 1% NP40, 0.5% sodium deoxycholate, 0.1% SDS, 1 mmol L^{-1} PMSF, 2 μg mL^{-1} aprotinin and 2 μg mL^{-1} leupeptin). The lysates were gently shaken at 4°C for 1 h, and the supernatants were collected. Proteins were then isolated by sodium dodecyl sulfate polyacrylamide gel electrophoresis (SDS-PAGE) and transferred to polyvinylidene difluoride (PVDF) membranes (Thermo Scientific, Rockford, IL, USA). The glyceraldehyde 3-phosphate dehydrogenase (GAPDH) protein was used as a reference. The membranes were blocked with Tris-buffered saline (TBS) supplemented with 0.1% Tween 20 and 5% BSA (TTBS-BSA), followed by incubation with mouse HIRRP anti-serum (1∶1000 dilution) at 4°C overnight. The membranes were washed three times in TTBS and incubated with HRP-anti-mouse IgG (1∶20000, Jackson, West Grove, PA, USA) at room temperature for 60 min. X-ray autoradiography was conducted in accordance with the manufacturer's instructions. Semi-quantitation using images was conducted with GelPro 3.1 (Media Cybernetics, MD, USA). The antiserum against HIRRP was raised in BALB/c mice immunized twice with the fusion of that protein and glutathione S-transferase (GST).

1.9 Yeast two-hybrid assays

AH109 yeast (Clontech, Palo Alto, CA, USA) transformed with recombinant pGBKT7-HIRRP was plated onto agar containing an SD/-Ade, SD/-His, SD/-Leu or SD/-Trp deficient medium and incubated at 30°C for 5–7 d. The AH109 (BD-HIRRP) culture was incubated with 1 mL of a human liver AD-cDNA library culture (Clontech, S1334, Lot 6010080) at 30°C overnight. The cells were shaken at 30–50 r min^{-1} on a platform shaker for 24 h. Aliquots (100 μL) of the fused mixture were serially diluted 10-fold (1∶10–1∶10000) and seeded onto plates containing SD/-Leu, SD/-Trp, SD/-Leu or SD/-Trp. The remaining mixtures were plated onto TDO (SD/-His/-Leu/-Trp) and QDO (SD/-Ade/-His/-Leu/-Trp) agar, followed by reverse cultivation at 30°C until positive clones appeared. The positive clones were amplified in liquid medium to measure the β-galactosidase activity using pGADT7-T and pGBKT7-p53 as positive controls, and pGADT7 and pGBKT7 as negative controls.

1.10 β-galactosidase activity

The recombinant pGBKT7 plasmid containing *hirrp* (or its N- or C-terminal fragment) and the recombinant pGADT7 plasmid containing *atf5* (or its C-terminal fragment) were co-transfected into AH109 yeast cells. Positive clones grown on QDO plates were screened and then cultivated with gentle shaking (200 r min^{-1}) at 30°C for 36 h. The yeast cells were lysed after centrifugation and separated into three aliquots. Fresh ortho-nitrophenyl-β-galactoside (ONPG) was added to each aliquot, and the samples were incubated at 30°C until the solutions were yellow; β-galactosidase activity was then calculated. Combinations of pGBKT7 and pGADT7 with pGBKT7-p53 and pGADT7-T were used as negative and positive controls, respectively. Each experiment was repeated five times, and the data were analyzed with GraphPad Prism 4.0. The values presented are mean±SE of five replicate samples.

1.11 Co-immunoprecipitation

Transfected and HSV-1-infected cells were collected and lysed in RIPA buffer with gentle shaking at 4°C for 1 h. The supernatants were collected, and protein A agarose (Sigma, St Louis, MO, USA) was used to capture the antigen-antibody complexes. The bound proteins were then separated by SDS-PAGE and analyzed by Western blotting [14].

1.12 Electrophoretic mobility shift assays (EMSAs)

A nuclear protein lysis solution (Pierce, Rockford, IL, USA) was applied to transfected L02 cells at 48 h post-transfection, in accordance with the standard EMSA protocol for 6%–8% non-denaturing gel electrophoresis using biotin-labeled DNA probes. The lysate was incubated at room temperature for 30 min and then transferred to a nylon membrane and cross-linked using UV light for 10 min. The membranes were blocked with an EMSA-specific blocking solution at room temperature for 30 min. Peroxidase-labeled streptavidin (SAP, 1∶500) was used to label the membranes, which were then subjected to X-ray autoradiography.

1.13 RNA interference (RNAi) assays

L02 cells transfected with RNAi fragments (Table 1) were infected with HSV-1 at an MOI of 0.1 at 24 h post-transfection. The total cellular RNA was then extracted at 36 hpi and reverse-transcribed into cDNA (Promega, Madison, WI, USA) following standard protocols. The resulting cDNA was stored at −20°C until required. The mRNA levels of ICP0, TK, gC, gB, and β-actin were determined using specific primers (Table 1) in qPCR assays. The data were analyzed using the $2^{-\triangle\triangle C_T}$ method.

2 Results

2.1 Up-regulated expression of HIRRP is induced in HSV-1-infected cells

We examined the possible correlation between the expression of HIRRP and HSV-1 infection (Figure S1 in Supporting Information). Interestingly, there was a significant up-regulation of *hirrp* mRNA in HSV-1- infected L02 cells at 6 hpi compared with that in uninfected cells (Figure 1A). This result was confirmed using qPCR assays, with mRNA levels in the infected cells increasing from 6 hpi (Figure 1B) and reaching 10-fold higher levels than in the control cells. Persistent expression of HIRRP was detected over the same period using Western blot assays (Figure 1C).

2.2 Localization of HIRRP

The subcellular localization of HIRRP was examined using green fluorescent protein (GFP)-tagged recombinant HIRRP. Our results showed that GFP-HIRRP was initially localized to the cytoplasm (Figures 2 and S2A in Supporting Information) and then partially translocated to the nucleus in HSV-1-infected cells (Figure 2). To confirm this observation, we analyzed the localization of native HIRRP in HSV-1-infected L02 cells. HIRRP was observed in the cytoplasm of HSV-1-infected L02 cells and then in the nucleus as infection progressed (Figure S2B in Supporting Information).

2.3 HIRRP can inhibit HSV-1 replication

The up-regulation of HIRRP was observed in HSV-1-infected L02 cells, and the expression of HIRRP in trans-

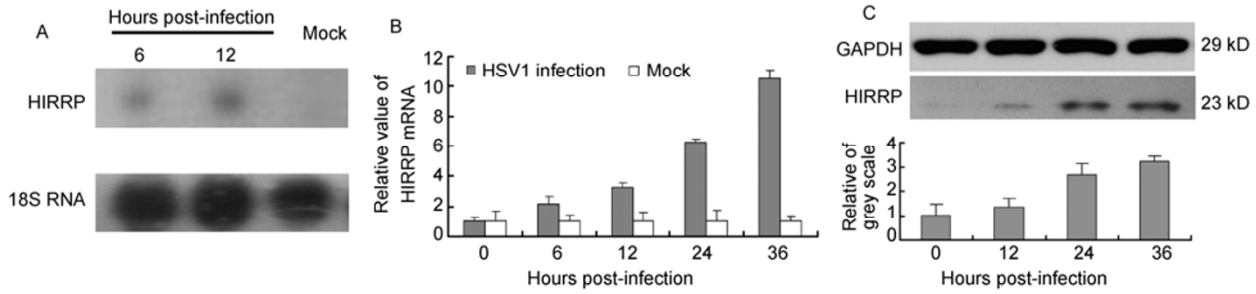

Figure 1 HIRRP expression is up-regulated during HSV-1 infection in L-02 cells. A, Northern blots were used to analyze HIRRP expression following HSV-1 infection of L-02 cells. The total RNA from HSV-1-infected L-02 cells was used for Northern blot analysis. A 60-nt fragment was identified (nt 121–180). B, Levels of *hirrp* mRNA detected by qPCR. C, Western blot assays were used to detect HIRRP in HSV-1-infected L-02 cells.

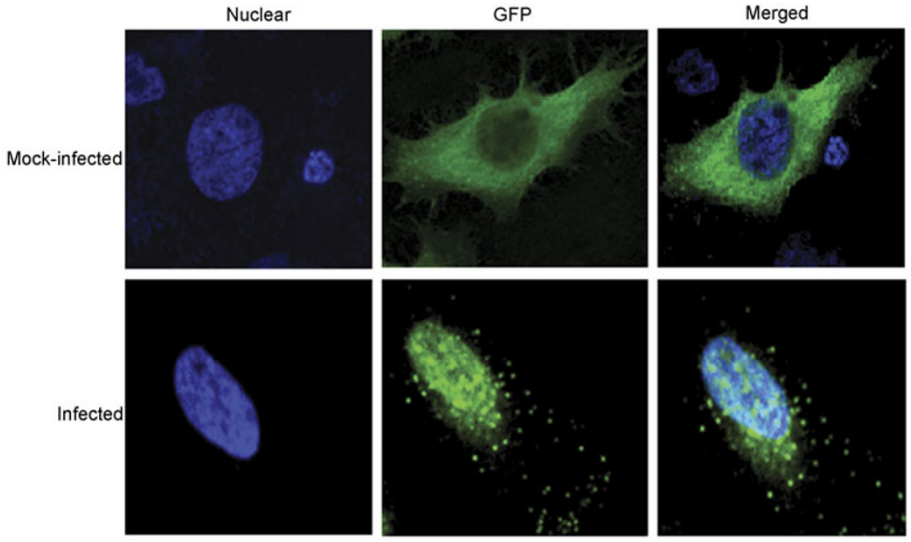

Figure 2 HIRRP translocates from the cytoplasm to the nucleus in HSV-1-infected cells. L-02 cells were transfected with pEGFP-HIRRP and then infected with HSV-1. Assays were conducted at 36 hpi. Mock-infected, cells transfected with pEGFP-HIRRP and uninfected; infected, cells transfected with pEGFP-HIRRP and infected with HSV-1. Nuclei were stained with Hoechst 33258 (blue).

fected cells reduced the replication efficiency of HSV-1 approximately 24 hpi (Figure 3A). The up-regulated expression of HIRRP inhibited the transcription of the *ICP0*, *TK* and *gC* genes (Figure 3B–D). The inhibitory effect on ICP0 was most obvious and occurred within 6 hpi (Figure 3B), and the inhibition of *TK* and *gC* transcription occurred within 8–12 hpi (Figures 3C and D). These inhibitory effects were not observed in cells co-transfected with eukaryotic expression vectors expressing the *ICP0*, *TK*, *gC* or *HIRRP* genes (Figure S3A–D in Supporting Information).

2.4 Knocking-down HIRRP expression improves HSV-1 replication efficiency

Next, the expression of hirrp was down-regulated using *hirrp*-specific microRNAs. Potential microRNA target sites in *hirrp* were identified using bioinformatics techniques, and three target sites were chosen (Figure S4A in Supporting Information). The miRNA-3 molecule significantly down-regulated *hirrp* transcription (Figure S4B in Supporting Information). In view of this down-regulation, the mRNA levels of *ICP0*, *TK*, *gC* and *gB* were examined at 12 hpi in HSV-1-infected cells. Compared with the controls, miRNA-3 enhanced the transcription of all HSV-1 genes while knocking-down *hirrp* expression levels (Figure 4A). Virus titration assays conducted at 24, 36 and 48 hpi showed that viral replication efficiency increased dramatically when HIRRP expression was blocked by miRNA-3 (Figure 4B).

2.5 HIRRP represses viral replication by interacting with ATF5

The yeast-two hybrid system allowed us to identify several proteins that potentially interact with HIRRP, including the transcription factor ATF5. We then examined the interaction between HIRRP and ATF5 using co-immunoprecipitation. HIRRP and ATF5 were co-precipitated in cells transfected with either exogenous *hirrp* or *atf5* (Figure 5A). HIRRP and ATF5 co-precipitated in HSV-1-infected cells (Figure 5B), and these results were confirmed by Western blotting. We found that the N-terminal domain of HIRRP bound to ATF5, whereas the C-terminal domain of ATF5 did not bind to HIRRP (Figure S5A and B in Supporting

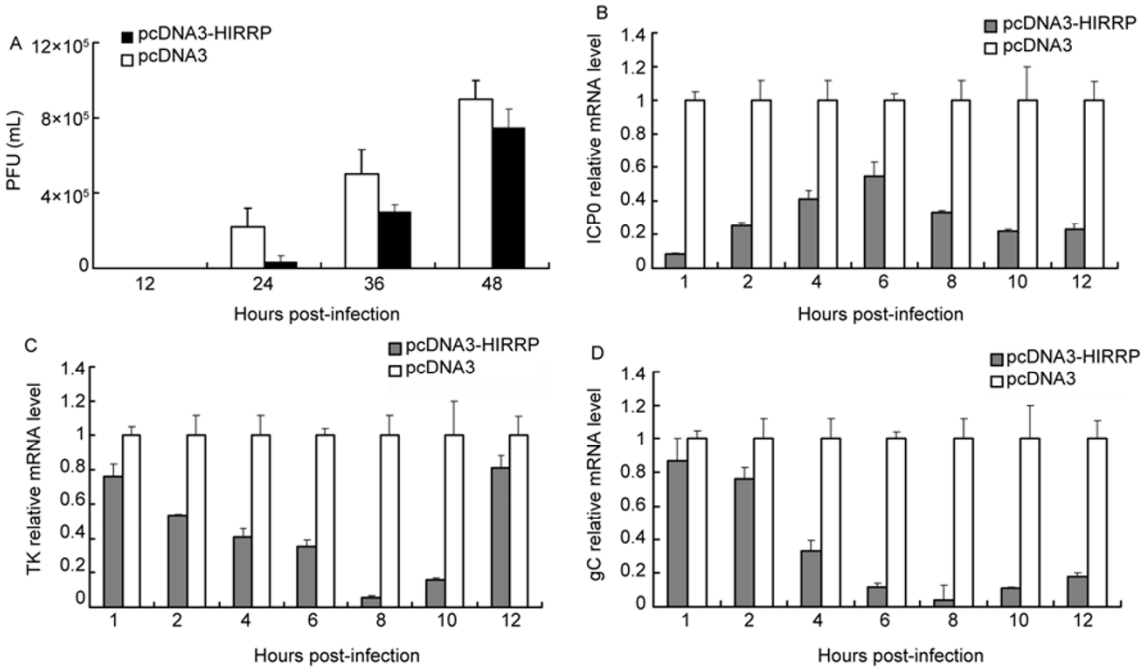

Figure 3 The overexpression of HIRRP inhibits HSV-1 replication. A, HIRRP expression affects HSV-1 proliferation in L-02 cells. Virus titration was conducted at 12, 24, 36, and 48 hpi. B, qPCR analysis of ICP0 gene expression in L-02 cells transfected with HIRRP. C, qPCR analysis of TK gene expression in L-02 cells transfected with HIRRP. D, qPCR analysis of gC gene expression in L-02 cells transfected with HIRRP.

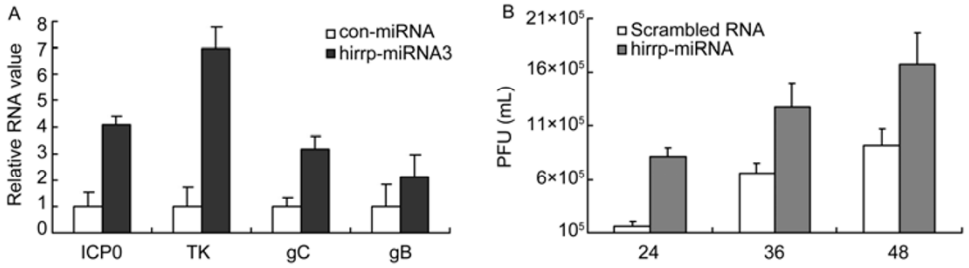

Figure 4 Down-regulating HIRRP expression in cells increases HSV-1 replication efficiency. A, The mRNA levels of ICP0, TK, gC and gB were increased upon down-regulation of *hirrp* expression. The viral genes were detected by qPCR. B, Virus titration was conducted at 24, 36 and 48 hpi.

Information). The *hirrp* deletion mutant DNA and *atf5* were then co-transfected into cells that were subsequently infected with HSV-1. The growth dynamics of HSV-1 in these cells was analyzed using plaque assays (Figure 5C). Viral replication was repressed in cells transfected with the N-terminal region of *hirrp* and *atf5* and in the positive control cells transfected with the whole *hirrp* expression plasmid. In contrast, the viral replication profile of cells transfected with the C-terminal region of *hirrp* and *atf5* was similar to that of the negative control cells (Figure 5C). We observed an interaction between the HIRRP N-terminal peptide (17.9 kD) and ATF5 using co-immunoprecipitation and Western blotting in cells co-transfected with the *hirrp* N-terminal region and the *atf5* gene. This result was consistent with the results obtained for control cells transfected with the complete *hirrp* gene (Figure 5D). In contrast, co-immunopre- cipitation was not detected with cells transfected with the *hirrp* C-terminal region (Figure 5D).

2.6 HIRRP blocks ATF5 from binding to a specific motif in the viral RL2 gene

The replication of HSV-1 was improved in L02 cells when ATF5 expression was up-regulated (Figure 6A). As a cellular transcription factor, ATF5 binds to up-stream response elements to regulate gene expression. Recent studies have revealed that ATF5 can bind to a specific motif (CCTCTTCCTTA) and activate transcription [33]. As indicated in the whole genome analysis of the HSV-1 F strain, this motif is located at nucleotides 2921–2928, 4797–4804, 4812–4819, 4848–4855, 12787–12794, 92762–92769 and 121562–121569 (within the *ICP0*, *UL5*, *UL41* and *UL42* genes; Figure S6 in Supporting Information). Considering the interaction between ATF5 and HIRRP, we next used EMSA to investigate the status of ATF5 binding to the specific motif (CCTCTTCCTTA) in the presence and absence

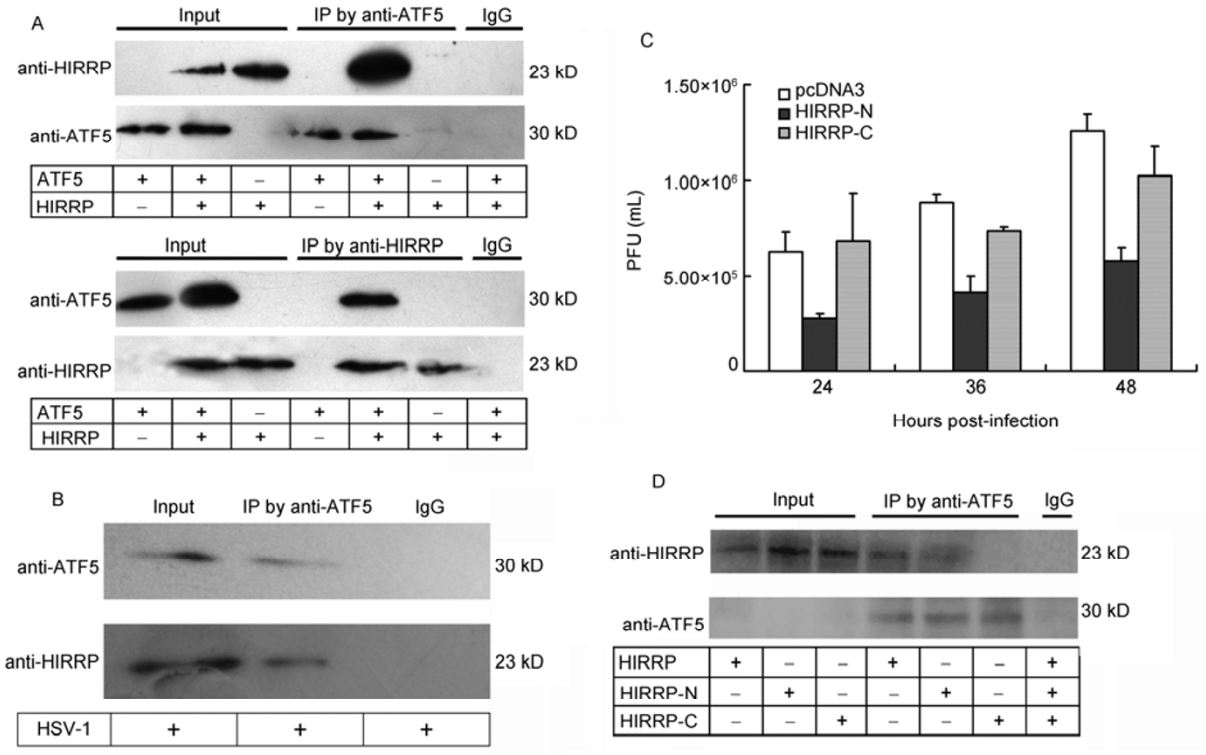

Figure 5 HIRRP inhibits viral replication by interacting with ATF5. A, Co-immunoprecipitation confirmed the interaction between HIRRP and ATF5. L-02 cells were transfected with pcDNA3-ATF5 and/or pcDNA3-HIRRP. The complex was precipitated with antibodies to ATF5 (upper panel) or HIRRP (lower panel). B, Co-immunoprecipitation assay on HSV-1-infected cells. L-02 cells were infected with HSV-1. The complex was precipitated with an ATF5-specific antibody. C, Dynamics of virus growth during HSV-1 infection when the N- or C-terminus of HIRRP was deleted. The *hirrp* deletion mutants and *atf5* were co-transfected into cells that were subsequently infected with HSV-1. Viral proliferation at 24, 36 and 48 hpi was assayed by titration. D, Co-immunoprecipitation confirmed the interaction between the N-terminus of HIRRP and ATF5. L-02 cells were transfected with pcDNA3-HIRRP, pcDNA3-HIRRP-N or pcDNA3-HIRRP-C. The complex was precipitated with an antibody to ATF5.

of HIRRP. Our results indicate that the retardation of labeled DNA fragments containing the specific motif occurred with eukaryotic cells expressing ATF5 alone, whereas no such binding was observed with cells co-expressing HIRRP and ATF5 (Figure 6C). These results indicate that ATF5 has the capacity to bind to the CCTCTTCCTTA motif (Figure 6B), whereas HIRRP can block this binding. However, determining whether this binding is directly linked to promoting transcriptional activation requires further investigation.

We therefore cloned the specific motif and its downstream 3.4 kb region from the HSV-1 genome into a eukaryotic expression vector, pcDNA3, for transfection into human L02 cells. As shown by 2-D electrophoresis, no protein products were expressed in L02 cells transfected with pcDNA3 compared with control cells (data not shown). We designed 10 probes for Northern blot analysis, each representing a 340-bp fragment, to scan for potential RNA transcription products within transfected cells. We detected one RNA transcript (370 nt; Figure 6D), indicating that transcription promoted by the specific motif could generate at least one RNA molecule of as-yet unknown function. Further experiments comparing the levels of this RNA molecule in cells with up- and down-regulated HIRRP expression suggested a correlation between the expression levels of this RNA and HIRRP (Figure 6E). We were able to identify this RNA molecule as a transcript of the HSV-1 genome (Figure 6F).

3 Discussion

Characterizing events during HSV-1 infection has enabled us to identify new cellular molecules involved in combating these infections [28]. HIRRP is a cellular response molecule that is up-regulated in HSV-1-infected cells and has been linked to the repression of viral replication. Here, we show that the overexpression of HIRRP reduces the replication efficiency of HSV-1 and the mRNA levels of its α, β and γ genes (Figure 3). In line with these results, the knock-down of *hirrp* enhanced the HSV-1 replication efficiency and the transcription of viral genes (Figure 4). By contrast, HIRRP overexpression did not impair the expression of the α, β and γ genes in transfected cells (Figure S3 in Supporting Information). The antiviral function of HIRRP appears to occur at the viral genome level; this notion is consistent with the

observation that HIRRP translocates from the cytoplasm to the nucleus during HSV-1 infection (Figure 2). Our findings suggest that HIRRP affects HSV-1 replication by binding to the N-terminus of ATF5 (Figures 5; Table S1, Figure S5 in Supporting Information). ATF5 has been reported to regulate viral transcription by binding to specific DNA fragments via a leucine zipper motif [34]. These binding sites have been identified as the CRE motif (TgAgCT) and are present in non-coding regions of the HSV-1 α gene [35]. Most reports have shown that ATF5 exerts an inhibitory effect on transcription after binding to CRE motifs [36], suggesting a potential inhibitory effect on HSV-1 gene transcription. In our study, HSV-1 replication in cells was enhanced when the expression of ATF5 was up-regulated with pcDNA3-ATF5 (Figure 6A). Our findings also suggest that the transcription of the *ICP0* gene, which has a similar CRE motif, was not affected by HIRRP inhibition. *ICP0* transcription and viral replication were inhibited following HSV-1 infection (Figures 3A and S3 in Supporting Information). Furthermore, ATF5 has been reported to bind to a specific DNA motif (CCTCTTCCTTA) and initiate the transcription of downstream sequences [33]. This motif is present in the HSV-1 RL2 gene and in other regions (Figure 6B). As shown by EMSA, ATF5 bound to this motif but lost this binding ability in the presence of HIRRP (Figure 6C). These results imply that ATF5 activates transcription by binding to a specific motif in the viral DNA. This is presumed to be significant in enhancing viral transcription. The interaction between HIRRP and ATF5 causes ATF5 to lose its capacity to bind to this motif, thereby impairing the transcription of viral genes and the replication of the virus. The analysis of the 3.4 kb downstream sequence of the specific motif (CCTCTTCCTTA) revealed that its associated protein and RNA molecules were expressed. The binding of ATF5 to this DNA motif induced the transcription of an RNA molecule rather than viral proteins (Figure 6C). We propose a putative genomic transcription model, in which during HSV-1 infection, the binding of ATF5 to a specific DNA motif (CCTCTTCCTTA) induces the expression of an RNA molecule from the 3.4 kb viral sequence; this RNA, in turn, causes enhanced transcriptional activation of the viral genome. According to previous reports, the transcriptional activation of HSV-1 is initiated by the VP16-Oct1-HCF complex. The results of this study reveal an important RNA molecule that is produced by the activation of viral transcription by cellular transcription factors and that interacts with HIRRP. We have provided new insights into the mechanisms of transcriptional regulation for the HSV-1 genome. However, the mechanisms by which this RNA molecule enhances transcription and possibly interacts with the VP16-Oct1-HCF complex require further investigation.

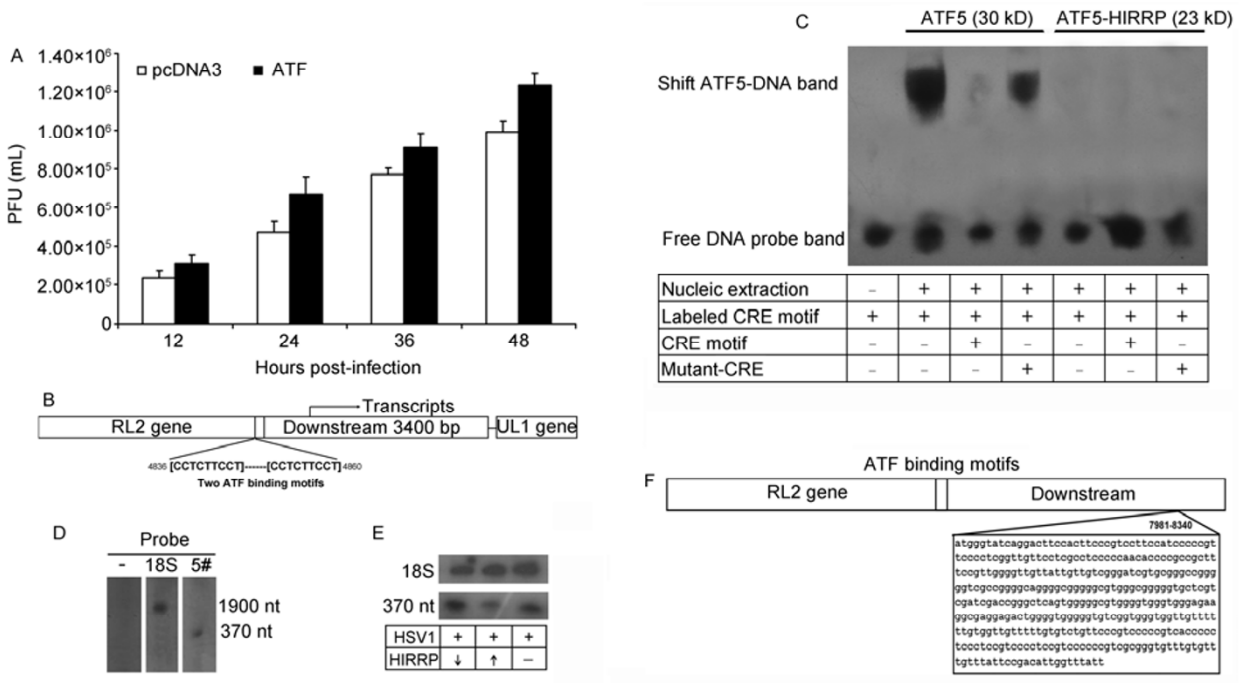

Figure 6 ATF5 binding to motifs in the RL2 gene activates transcription. A, Up-regulating the expression of ATF5 can increase HSV-1 replication efficiency. Virus titration was conducted for cells transfected with pcDNA3-ATF5 and/or pcDNA3 at 12, 24, 36, 48 hpi. B, Two specific motifs located within the RL2 gene are recognized by ATF5. C, EMSA to determine the DNA-binding capacity of ATF5 in cells co-transfected with ATF5 and HIRRP. L-02 cells were transfected with pcDNA3-ATF5 and/or pcDNA3-HIRRP. D, Northern blot analysis of transcripts regulated by the ATF5 binding motifs in the RL2 gene. The 18S rRNA was used as an internal control. E, Expression analysis showed a 370-nt RNA that is correlated with HIRRP levels. The expression of *hirrp* was reduced following HSV-1 infection using the *hirrp*-specific miRNA-3. The 18S rRNA was used as an internal control. F, An RNA molecule bound to the 370-nt motif was identified in the virus genome.

This work was supported by the National Basic Research Program of China (2012CB518901) and the National Natural Science Foundation of China (31100127).

1 Negorev D G, Vladimirova O V, Maul G G. Differential functions of interferon-upregulated Sp100 isoforms: Herpes simplex virus type 1 promoter-based immediate-early gene suppression and PML protection from ICP0-mediated degradation. J Virol, 2009, 83: 5168–5180
2 Servant M J, Grandvaux N H J. Multiple signaling pathways leading to the activation of interferon regulatory factor 3. Biochem Pharmacol, 2002, 64: 985–992
3 Kim J C, Lee S Y, Kim S Y, et al. HSV-1 ICP27 suppresses NF-kappaB activity by stabilizing IkappaBalpha. FEBS Lett, 2008, 582: 2371–2376
4 Lin R, Noyce R S, Collins S E, et al. The herpes simplex virus ICP0 RING finger domain inhibits IRF3- and IRF7-mediated activation of interferon-stimulated genes. J Virol, 2004, 78: 1675–1684
5 Fossum E, Friedel C C, Rajagopala SV, et al. Evolutionarily conserved herpesviral protein interaction networks. PLoS Pathog, 2009, 5: e1000570
6 Uetz P, Dong Y A, Zeretzke C, et al. Herpesviral protein networks and their interaction with the human proteome. Science, 2006, 311: 239–242
7 McGavern D B, Kang S S. Illuminating viral infections in the nervous system. Nat Rev Immunol, 2011, 11: 318–329
8 Cliffe A R, Garber D A, Knipe D M. Transcription of the herpes simplex virus latency-associated transcript promotes the formation of facultative heterochromatin on lytic promoters. J Virol, 2009, 83: 8182–8190
9 Divito S, Cherpes T L, Hendricks R L. A triple entente: Virus, neurons, and $CD8^+$ T cells maintain HSV-1 latency. Immunol Res, 2006, 36: 119–126
10 Cun W, Guo L, Zhang Y, et al. Transcriptional regulation of the Herpes simplex virus 1alpha-gene by the viral immediate-early protein ICP22 in association with VP16. Sci China Ser C-Life Sci, 2009, 52: 344–351
11 Yu X, Li W, Liu L, et al. Functional analysis of transcriptional regulation of herpes simplex virus type 1 tegument protein VP22. Sci China Ser C-Life Sci, 2008, 51: 966–972
12 Guo H, Cun W, Liu L, et al. Immediate-early gene product ICP22 inhibits the trans-transcription activating function of P53-mdm-2. Sci China Ser C-Life Sci, 2007, 50: 473–478
13 Wu W, Yu X, Li W, et al. HSV-1 stimulation-related protein HSRG1 inhibits viral gene transcriptional elongation by interacting with Cyclin T2. Sci China Life Sci, 2011, 54: 359–365
14 Yu X, Liu L, Wu L, et al. Herpes simplex virus type 1 tegument protein VP22 is capable of modulating the transcription of viral TK and gC genes via interaction with viral ICP0. Biochimie, 2010, 92: 1024–1030
15 Herrera F J, Triezenberg S J. VP16-dependent association of chromatin-modifying coactivators and underrepresentation of histones at immediate-early gene promoters during herpes simplex virus infection. J Virol, 2004, 78: 9689–9696
16 Wysocka J, Herr W. The herpes simplex virus VP16-induced complex: The makings of a regulatory switch. Trends Biochem Sci, 2003, 28: 294–304
17 Luciano R L, Wilson A C. An activation domain in the C-terminal subunit of HCF-1 is important for transactivation by VP16 and LZIP. Proc Natl Acad Sci USA, 2002, 99: 13403–13408
18 Nogueira M L, Wang V E, Tantin D, et al. Herpes simplex virus infections are arrested in Oct-1-deficient cells. Proc Natl Acad Sci USA, 2004, 101: 1473–1478
19 Cai W, Schaffer P A. Herpes simplex virus type 1 ICP0 regulates expression of immediate-early, early, and late genes in productively infected cells. J Virol, 1992, 66: 2904–2915
20 Millhouse S, Wigdahl B. Molecular circuitry regulating herpes simplex virus type 1 latency in neurons. J Neurovirol, 2000, 6: 6–24
21 Hong M, Che Y C, Tang G Z. Herpes simplex virus 1 infection alters the mRNA translation processing in L-02 cells. Virol Sin, 2008, 23: 43–50
22 Christensen T. Association of human endogenous retroviruses with multiple sclerosis and possible interactions with herpes viruses. Rev Med Virol, 2005, 15: 179–211
23 Umbach J L, Nagel M A, Cohrs R J, et al. Analysis of human alphaherpesvirus microRNA expression in latently infected human trigeminal ganglia. J Virol, 2009, 83: 10677–10683
24 Roberts A P, Abaitua F, O'Hare P, et al. Differing roles of inner tegument proteins pUL36 and pUL37 during entry of herpes simplex virus type 1. J Virol, 2009, 83: 105–116
25 Lagos D, Pollara G, Henderson S, et al. miR-132 regulates antiviral innate immunity through suppression of the p300 transcriptional co-activator. Nat Cell Biol, 2010, 12: 513–519
26 Akhtar J, Shukla D. Viral entry mechanisms: Cellular and viral mediators of herpes simplex virus entry. FEBS J, 2009, 276: 7228–7236
27 Guo H X, Cun W, Liu L D, et al. Protein encoded by HSV-1 stimulation-related gene 1 (HSRG1) interacts with and inhibits SV40 large T antigen. Cell Prolif, 2006, 39: 507–518
28 Dong S, Dong C, Liu L, et al. Identification of a novel human sand family protein in human fibroblasts induced by herpes simplex virus 1 binding. Acta Virol, 2003, 47: 27–32
29 Li Q, Zhao H, Jiang L, et al. An SR-protein induced by HSVI binding to cells functioning as a splicing inhibitor of viral pre-mRNA. J Mol Biol, 2002, 316: 887–894
30 Kawaguchi Y, Bruni R, Roizman B, et al. Interaction of herpes simplex virus 1 alpha regulatory protein ICP0 with elongation factor 1delta: ICP0 affects translational machinery. J Virol, 1997, 71: 1019–1024
31 Raczniak G A, Bulkow L R, Bruce M G, et al. Long-term immunogenicity of hepatitis A virus vaccine in Alaska 17 years after initial childhood series. J Infect Dis, 2013, 207: 493–496
32 Schmittgen T D, Livak K J. Analyzing real-time PCR data by the comparative C(T) method. Nat Protoc, 2008, 3: 1101–1108
33 Li G, Li W, Angelastro J M, et al. Identification of a novel DNA binding site and a transcriptional target for activating transcription factor 5 in C6 glioma and MCF-7 breast cancer cells. Mol Cancer Res, 2009, 7: 933
34 Persengiev S P, Devireddy L R, Green M R. Inhibition of apoptosis by ATFx: A novel role for a member of the ATF/CREBfamily of mammalian bZIP transcription factors. Genes Dev, 2002, 16: 1806–1814
35 Davido D J, Leib D A. Analysis of the basal and inducible activities of the ICPO promoter of herpes simplex virus type 1. J Gen Virol, 1998, 79: 2093–2098
36 Wang H, Lin G, Zhang Z. ATF5 promotes cell survival through transcriptional activation of Hsp27 in H9c2 cells. Cell Biol Int, 2007, 31: 1309–1315

Supporting Information

Figure S1 2-D analysis of HSV-1-infected human L-02 cells. A, 2-D electrophoresis analysis of mock-infected L-02 cells. B, 2-D electrophoresis analysis of HSV-1-infected L-02 cells. 'G' indicates a difference in protein expression identified in infected cells.

Figure S2 Localization and translocation of HIRRP in HSV-1-infected cells. A, Localization of HIRRP in Vero, Hela and 293T cells. Nuclei were stained with Hoechst 33258 (blue). B, Immunofluorescence assays were used to detect HIRRP expression in HSV-1-infected cells. The experiments were conducted at 36 hpi.

Figure S3 Inhibition of ICP0, TK and gC expression when co-transfecting their genes and HIRRP. A, Schematic of expression vectors for ICP0, TK and gC. B, qPCR analysis of ICP0 gene expression in L-02 cells co-transfected with HIRRP and ICP0 (including the 5′ terminus ICP0 promoter). C, qPCR analysis of TK gene expression in L-02 cells transfected with HIRRP and TK (including the 5′ terminus TK promoter). D, qPCR analysis of gC gene expression in L-02 cells transfected with HIRRP and gC (including the 5′ terminus gC promoter).

Figure S4 The miRNA-3 molecule down-regulates *hirrp* transcription. A, Three potential microRNA target sites in *hirrp* were predicted (blue, italicized). B, qPCR analysis of *hirrp* gene expression in L-02 cells knocked-down with miRNA-3.

Figure S5 Analysis of the interaction between HIRRP and ATF5 using a yeast two-hybrid assay system. A, Schematic of the HIRRP structural domains based on various deletion mutants. B, Binding analysis of HIRRP and ATF5 domains.

Figure S6 Schematic of DNA motifs identified in ATF5. IR, internal repeat; TR, terminal repeat; U_L, unique long; U_S, unique short.

The supporting information is available online at life.scichina.com and www.springerlink.com. The supporting materials are published as submitted, without typesetting or editing. The responsibility for scientific accuracy and content remains entirely with the authors.